Electronic Supplementary Material (ESI) for Journal of Materials Chemistry A.

High Cycle Stability of Zn Anode Boosted by An Artificial Electronic-Ionic Mixed Conductor Coating Layer

Weijia Fan[a], Zhenwen Sun[a], Ye Yuan[a], Xinhai Yuan[a], Chaolin You[a], Qinghong Huang[a], Jilei Ye[a], Lijun Fu*[a], Veniamin Kondratiev[b], Yuping Wu*[a]

a State Key Laboratory of Materials-Oriented Chemical Engineering, College of Energy Science and Engineering, and College of Chemical Engineering, Nanjing Tech University, Nanjing 211816, Jiangsu Province, China

b Department of Electrochemistry, Institute of Chemistry, Saint Petersburg State University, 7/9 Universitetskaya nab., St. Petersburg, 199034, Russi

Experimental Section

Preparation of the zinc anode

PVDF+AB@Zn: The slurry comprising Acidified carbon black (AB) (70wt%), and polyvinylidene fluoride (30wt%) in N-methyl-2-pyrrolidone was cast onto zinc foil. Then the as-prepared electrode was placed in a vacuum for 12 hours.

Alg-Zn@Zn: The sodium alginate (AR grade, Aladdin) was dissolved in deionized water at a weight ratio of 1:100 followed by stirring for 12 h. Then, the homogeneous sodium alginate solution was cast onto zinc foil, and then soaked in a solution of 2 M $ZnSO_4$ to achieve Alg-Zn@Zn.

Alg-Zn+AB@Zn: The Sodium alginate, AB is dissolved in water with the weight ratio of 3:7:300. The remaining steps are the same as Alg-Zn@Zn.

Preparation of V_2O_5[1]

1.5 g commercial V_2O_5 powder was mixed with 50 mL 2 M NaCl solution under stirring for 72 h at room temperature. The product was vacuum filtered and washed with ultrapure water and ethanol. Finally, the product was dried in at 70 °C for 12 h.

Characterization

The crystallographic structure was analyzed by X-ray diffractometer (XRD, D/MAX-IIA, Rigaku) with Cu-Kα radiation (λ = 0.15406 nm) at a scanning angle (2θ) range of 10° to 90°. The morphology and microstructure observation of the samples was measured by scanning electron microscopy (SEM, XL-70, Philips) and optical microscope (YM520R).

Electrochemical measurements

symmetrical batteries were tested using a glass fiber separator with Zn and Improved anodes (PVDF+AB@Zn, Alg-Zn@Zn and Alg-Zn+AB@Zn) in a CR2032 coin battery and assembled in the air. 2 M $ZnSO_4$ aqueous solution was used as the electrolyte. The electrolyte content is 60 μL.

After that, full cells were fabricated with Alg-Zn+AB@Zn and Activated Carbon (AC)/ V_2O_5. AC was mixed with Carbon Black (CB), and Polytetrafluoroethylene (PTFE) at a weight ratio of 8: 1: 1, and then the slurry dried under infrared baking lamp for 1 h. Then, the mixture was pressed onto stainless steel mesh. The mass of cathode is about 4 mg cm^{-2}.

The V_2O_5, Carbon Black, and PTFE binder were grinded at a mass ration of 7:2:1. The viscous mixture dried under infrared baking lamp for 1 h. Then, the mixture was pressed onto stainless steel mesh. The mass of cathode is about 4～8 mg cm^{-2}.

The electrochemical performance was implemented by a battery test system (LAND) at room temperature. The Cyclic voltammetry (CV) was recorded on an electrochemical workstation (CHI660E). Electrochemical Impedance Spectroscopy (EIS) was measured by an impedance/gain-phase analyzer (Solartron analytical 1260A) and an electrochemical test analyzer (Solartron analytical 1287A).

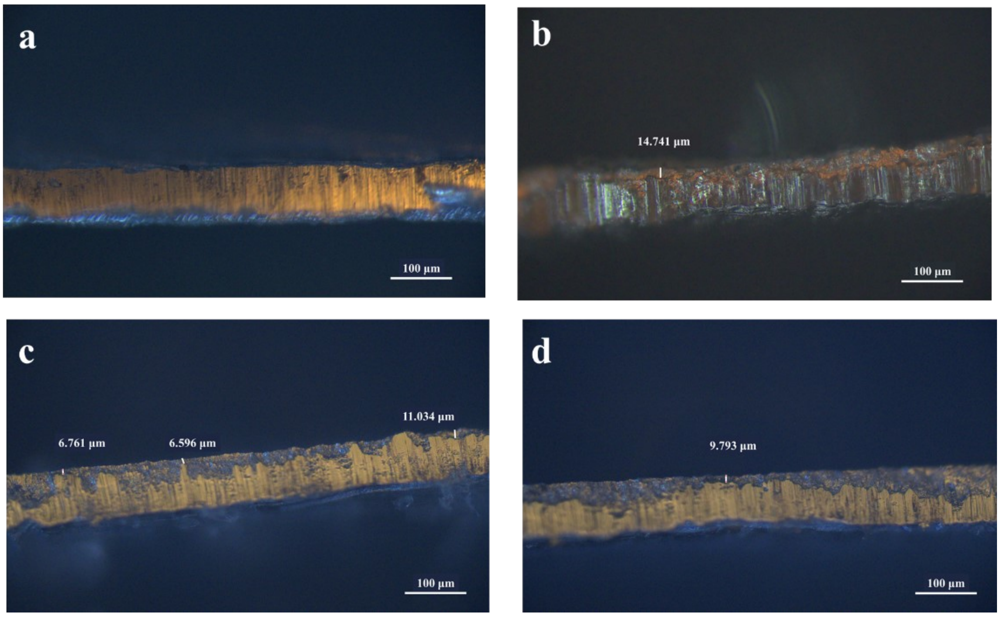

Fig. S1 The cross-sectional optical images of a) Zn, b) PVDF+AB@Zn, c) Alg-Zn@Zn and d) Alg-Zn+AB@Zn. The coating layers were immersed in the electrolyte to observe their thickness in the status of cycling.

The varied Alg-Zn coating thickness as shown in Fig. S1c and S1d is due to the extensible property of Alg-Zn, the thinnest part of coating layer is measured as the thickness of coating layer.

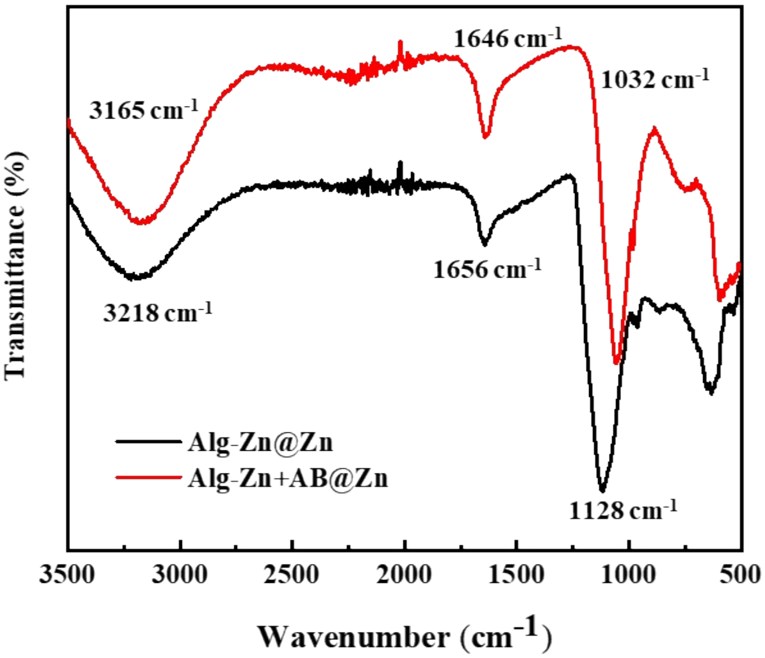

Fig. S2 FT-IR spectra of Alg-Zn@Zn and Alg-Zn+AB@Zn.

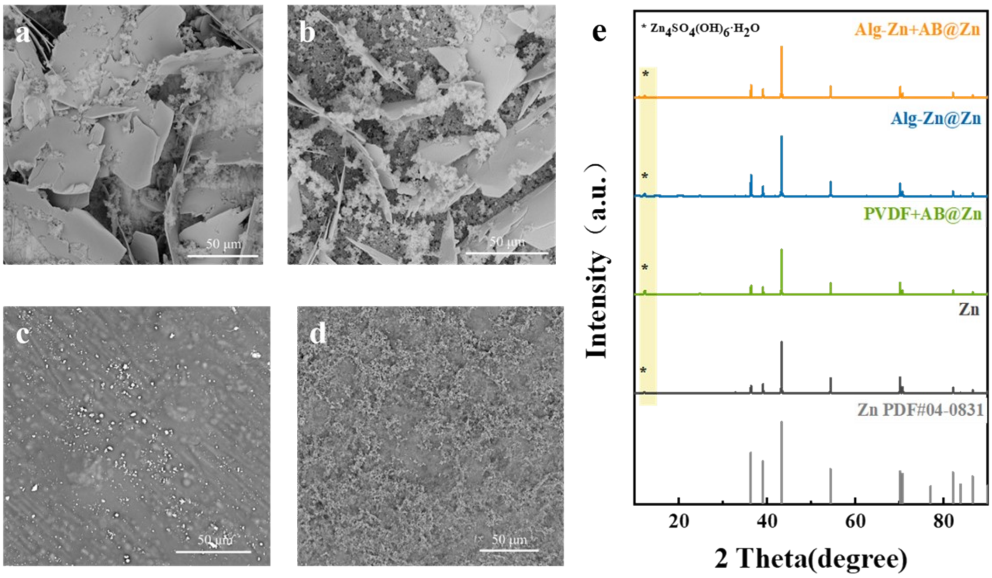

Fig. S3 Characterizations of the anode soaked in 2 M $ZnSO_4$ electrolyte for 7 days. SEM images of a) Zn, b) PVDF+AB@Zn, c) Alg-Zn@Zn and d) Alg-Zn+AB@Zn. e) XRD patterns.

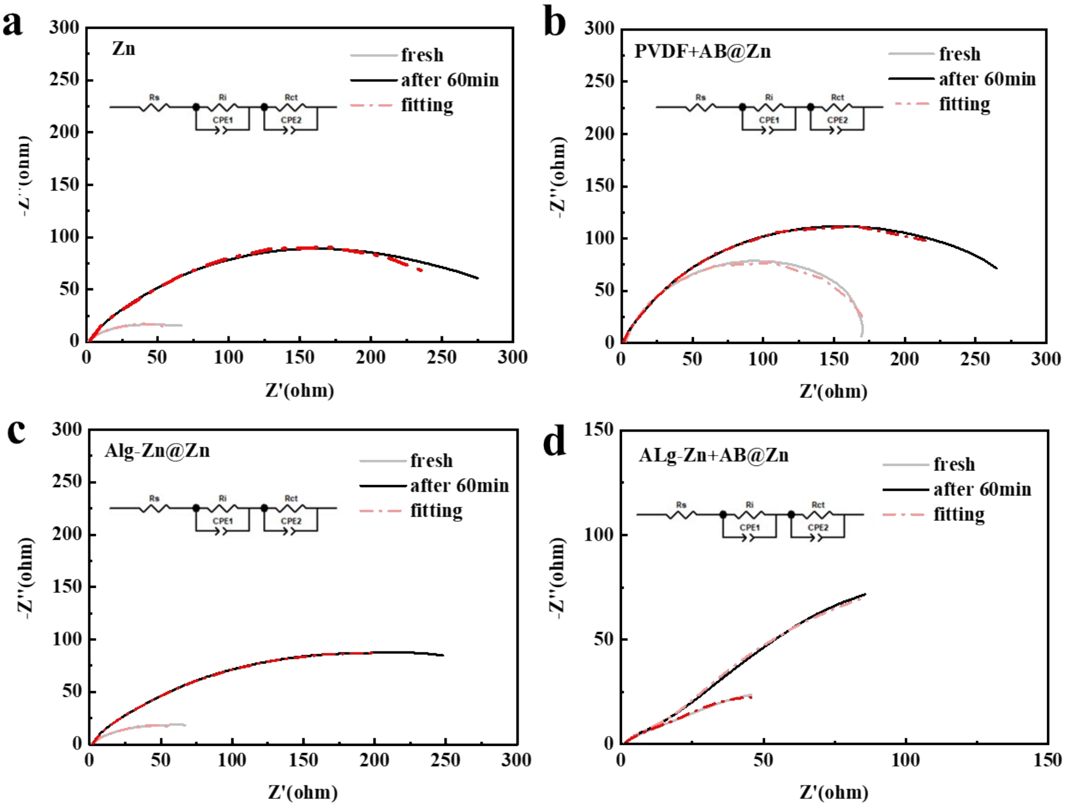

Fig. S4 EIS of a) Zn, b) PVDF+AB@Zn, c) Alg-Zn@Zn and d) Alg-Zn+AB@Zn before and after standing. The equivalent circuit to fit the EIS data, where Rs is series resistance; Ri is solid state electrolyte interface layer resistance between electrolyte and electrode; Rct is charge-transfer resistance; and CPE is constant-phase element.

Table 1 The corresponding resistance of symmetrical cells.

	Rs	Ri	Rct
Zn	0.95	12.36	59.06
Zn-1 h	1.87	15.89	282.8
PVDF+AB@Zn	2.116	0.77	183.9
PVDF+AB@Zn-1 h	1.05	7.05	288
Alg-Zn@Zn	1.12	9.38	70.04
Alg-Zn@Zn-1 h	1.99	26.96	273
Alg-Zn+AB@Zn	1.23	16.75	47.14
Alg-Zn+AB@Zn- 1 h	1.384	32.98	231.2

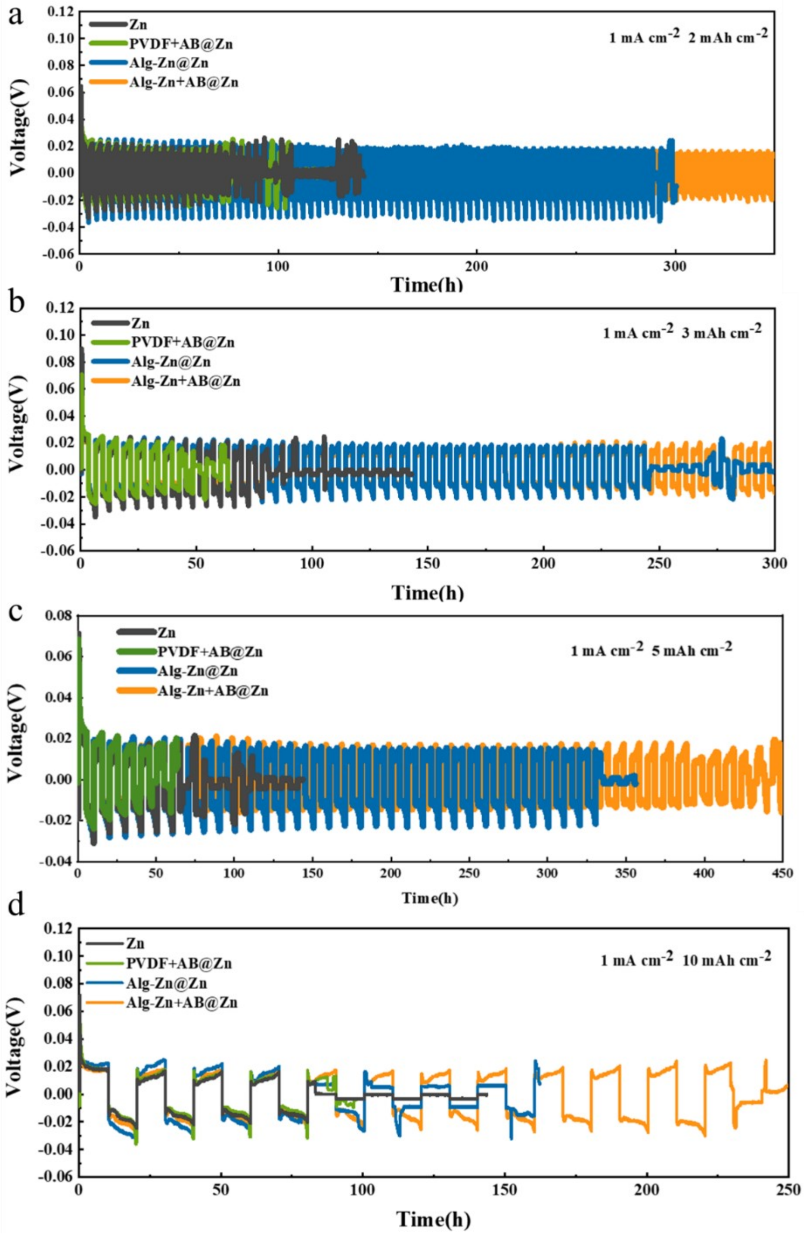

Fig. S5 Deep stripping/plating abilities of Zn, PVDF+AB@Zn, Alg-Zn@Zn and Alg-Zn+AB@Zn with areal capacities varying from 2 to 10 mA h cm^{-2} at a constant current density of 1 mA cm^{-2}.

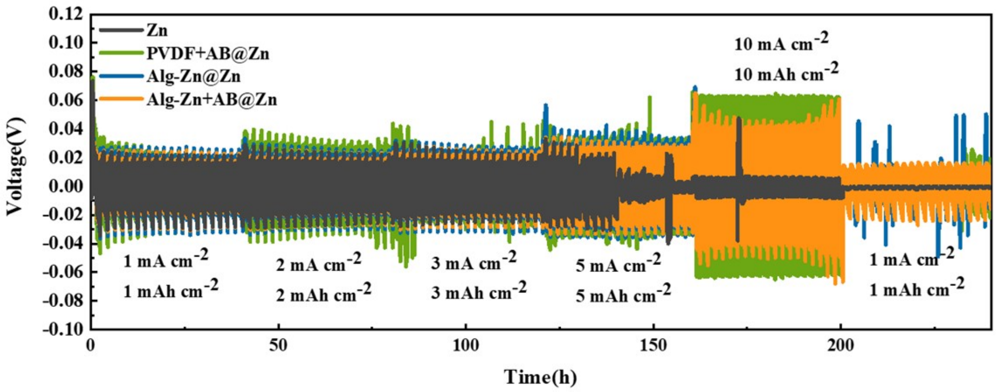

Fig. S6 Rate performances at current densities from 1 to 10 mA cm^{-2}.

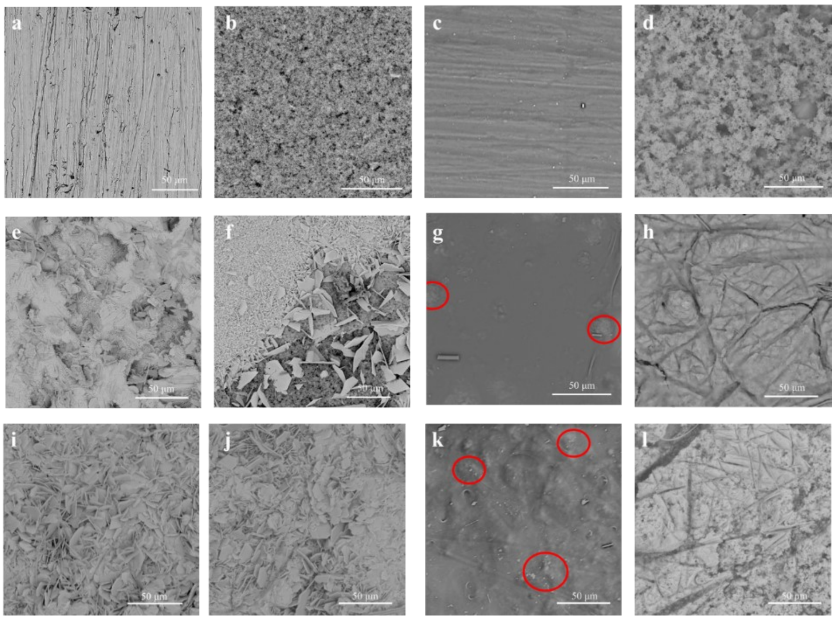

Fig. S7 Morphology and structure of different Zn anodes after cycled in symmetrical cells at a current density of 1 mA cm^{-2} and areal capacity of 1 mAh cm^{-2}. a) SEM images of bare Zn before cycling, e) after 20 cycles and i) short circuit. b) SEM image of PVDF+AB@Zn before cycling, f) after 20 cycles and j) after 50 cycles. c) SEM image of Alg-Zn@Zn before cycling, g) after 20 cycles and k) after 50 cycles. d) SEM image of Alg-Zn+AB@Zn before cycling, h) after 20 cycles and l) after 50 cycles. The scale bar in Fig. S6a-6l represents 50 μm.

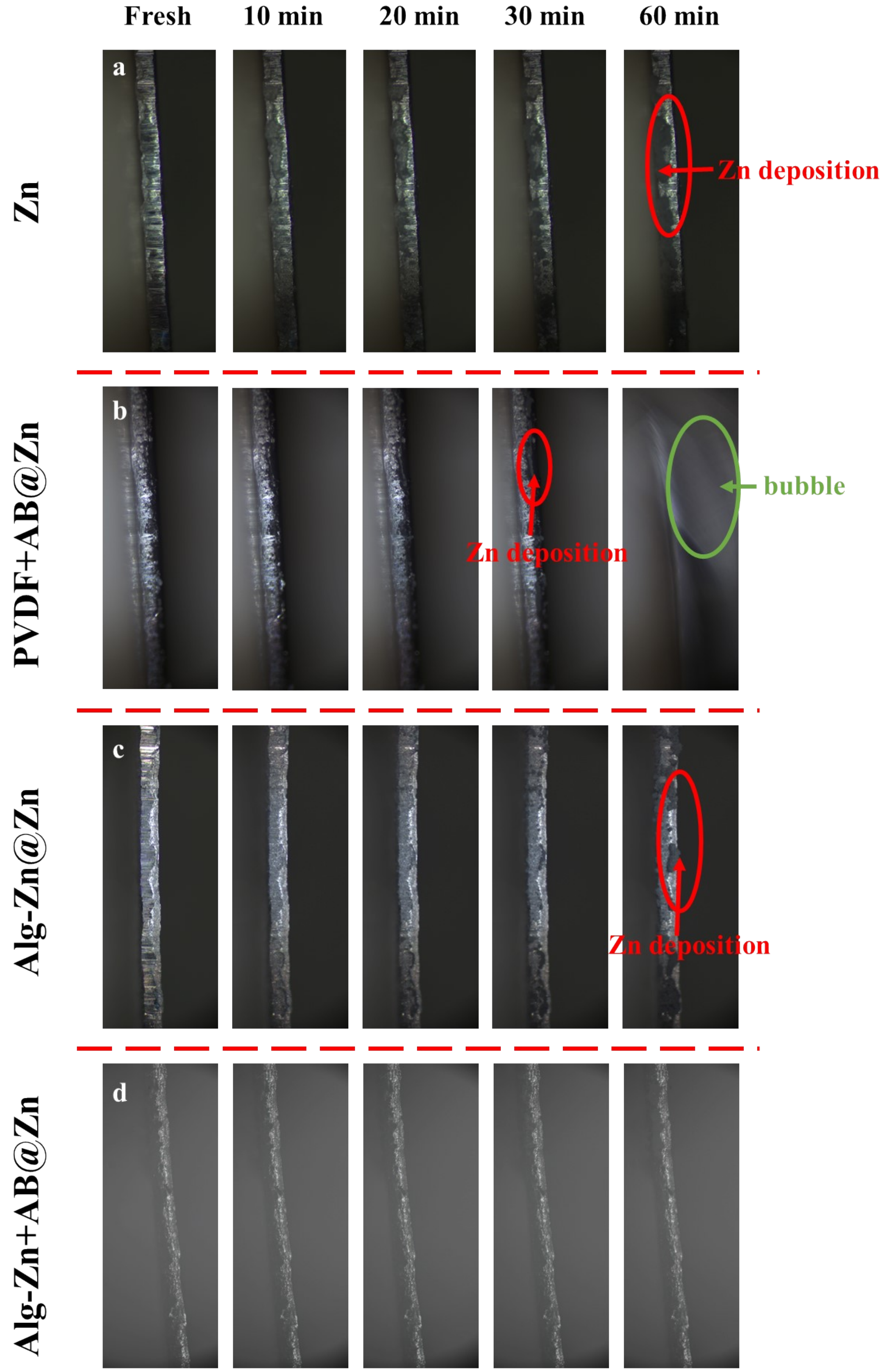

Fig. S8 In situ optical observation results of the Zn deposition morphologies on a) Zn, b) PVDF+AB@Zn, c) Alg-Zn@Zn, and d) Alg-Zn+AB@Zn at 0.1 mA cm^{-1}.

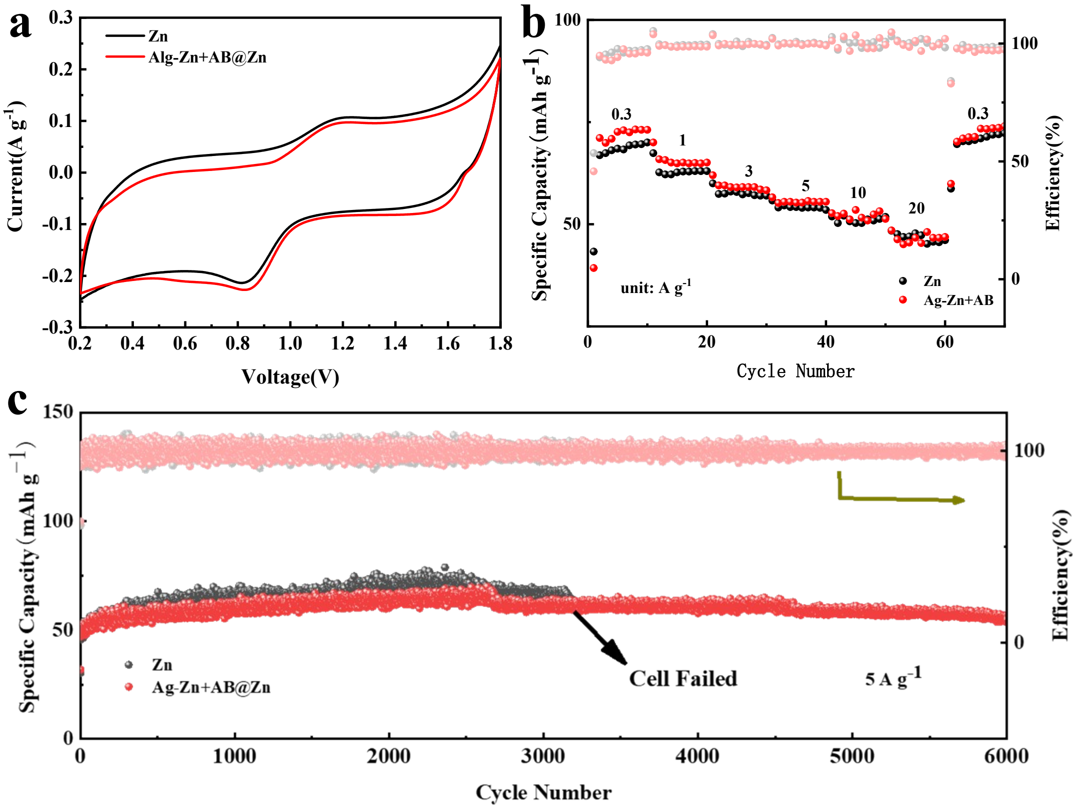

Fig. S9 Evaluation of Zn/AC full cells with bare Zn and Alg-Zn+AB@Zn as anodes. a) CV curves of bare Zn/AC and Alg-Zn+AB@Zn/AC full cells at 10 mV s^{-1}, the current density is calculated based on the mass of AC. b) rate capability of bare Zn/AC and Alg-Zn+AB@Zn/AC full cells ranging from 0.3 to 20 A g^{-1}, c) Cycling stability of bare Zn/AC and Alg-Zn+AB@Zn/AC full cells at 5 A g^{-1}.

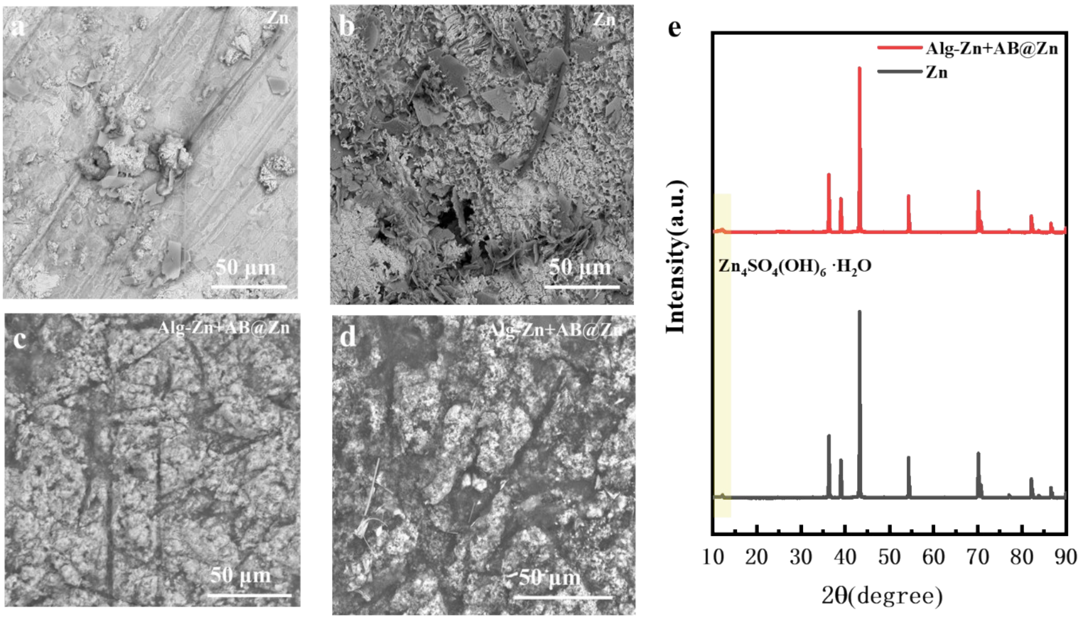

Fig. S10 Characterizations of the anode. SEM images recovered from Zn/AC full cells of a) Zn, c) Alg-Zn+AB@Zn after 200 plating/striping cycles at 5 A g^{-1}; b) Zn and d) Alg-Zn+AB@Zn after 1000 plating/striping cycles at 10 A g^{-1}. e) XRD patterns of Zn/Zn symmetrical cells after 1000 plating/striping cycles at 10 A g^{-1}.

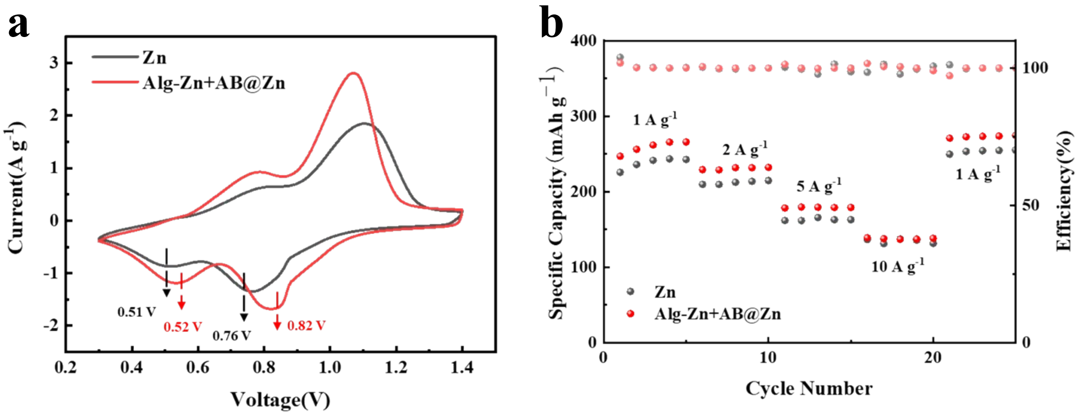

Fig. S11 Evaluation of Zn/V_2O_5 full celles with bare Zn and Alg-Zn+AB@Zn as anodes. a) CV images of bare Zn/ V_2O_5 and Alg-Zn+AB@Zn/V_2O_5 full cells at 1 mV s^{-1}, the current density is calculated based on the mass of V_2O_5; b) rate capability of bare Zn/ V_2O_5 and Alg-Zn+AB@Zn/ V_2O_5 full batteries ranging from 1 to 10 A g^{-1}.

Table. S2 Performance comparison of galvanostatic Zn stripping/plating of the reported Zn/Zn symmetrical cells.

Strategies	Current density (mA cm^{-2})	Areal capacity Operation (mAh cm^{-2})	Over potential (mV)	Operation cycles (h)	Reference
Zn@C	2.5	1	25	300	2
Zn/rGO	10	2	400	200	3
CM@CuO@Zn	1	1	11	340	4
PEDOT:PSS/GS@Zn	1	1		500	5
Zn|In	1	1	54	500	6
60alucone@Zn	1	1	46.1	498	7
Zn–G	0.1	0.1		200	8
Zn/CNT	2	2	27	100	9
ZF@CB-NFC	0.5	0.5	160	400	10
PA6/Zn(TfO)$_2$@Zn	0.5	1		450	11
Zn (002)	1	1	38	500	12
Janus Separator (MOF/rGO Interlayers)	2	1	89	500	13
Alg-Zn+AB@Zn	1	1	46	500	This work

Table. S3 Performance comparison of the reported Zn/AC cells.

Strategies	Current density (A g^{-1})	Operation cycles	Capacity retention	Reference
Zn@ZnF$_2$	2	5000	92.8%	14
poly(4,4′-TDP)	8	2000	71%	15
Janus Separator (vertical graphene)	5	5000	93.7%	16
Alg-Zn+AB@Zn	10	10000	~100%	This work
	20	16000	~100%	

References:

1. Y. Li, Z. Huang, P. K. Kalambate, Y. Zhong, Z. Huang, M. Xie, Y. Shen and Y. Huang, *Nano Energy*, 2019, **60**, 752-759.
2. W. Li, K. Wang, M. Zhou, H. Zhan, S. Cheng and K. Jiang, *ACS Appl. Mater. Interfaces*, 2018, **10**, 22059-22066.
3. C. Shen, X. Li, N. Li, K. Xie, J. G. Wang, X. Liu and B. Wei, *ACS Appl Mater Interfaces*, 2018, **10**, 25446-25453.
4. Q. Zhang, J. Luan, X. Huang, L. Zhu, Y. Tang, X. Ji and H. Wang, *Small*, 2020, **16**, 2000929.
5. M. Qiu, D. Wang, B. Tawiah, H. Jia, B. Fei and S. Fu, *Composites Part B: Engineering*, 2021, **215**, 108798.
6. D. Han, S. Wu, S. Zhang, Y. Deng, C. Cui, L. Zhang, Y. Long, H. Li, Y. Tao, Z. Weng, Q.-H. Yang and F. Kang, *Small*, 2020, 2001736.
7. H. He and J. Liu, *J. Mater. Chem. A*, 2020, **8**, 22100-22110.
8. Z. Li, L. Wu, S. Dong, T. Xu, S. Li, Y. An, J. Jiang and X. Zhang, *Adv. Funct. Mater.*, 2020, **31**, 2006495.
9. Y. Zeng, X. Zhang, R. Qin, X. Liu, P. Fang, D. Zheng, Y. Tong and X. Lu, *Adv. Mater. Processes*, 2019, **31**, 1903675.
10. A. Wang, W. Zhou, A. Huang, M. Chen, J. Chen, Q. Tian and J. Xu, *J. Colloid Interface Sci.*, 2020, **577**, 256-264.
11. J. Cui, Z. Li, A. Xu, J. Li and M. Shao, *Small*, 2021, **17**, 2100722.
12. M. Zhou, S. Guo, J. Li, X. Luo, Z. Liu, T. Zhang, X. Cao, M. Long, B. Lu, A. Pan, G. Fang, J. Zhou and S. Liang, *Adv. Mater.*, 2021, **33**, e2100187.
13. Z. Wang, L. Dong, W. Huang, H. Jia, Q. Zhao, Y. Wang, B. Fei and F. Pan, *Nanomicro Lett*, 2021, **13**, 73.
14. Yang Yang, Liu Chaoyue, Lv Zeheng, Yang Hao, Zhang Yufei, Ye Minghui, Chen Libao, Zhao Jinbao and L. ChengChao, *Adv. Mater.*, 2021, **33**, 2007388.
15. T. Xin, Y. Wang, N. Wang, Y. Zhao, H. Li, Z. Zhang and J. Liu, *J. Mater. Chem. A*, 2019, **7**, 23076-23083.
16. C. Li, Z. Sun, T. Yang, L. Yu, N. Wei, Z. Tian, J. Cai, J. Lv, Y. Shao, M. H. Rümmeli, J. Sun and Z. Liu, *Adv. Mater.*, 2020, **32**, 2003425.